

## Detection of Sub-surface Delamination and Moisture Penetration in Unlined Rock Tunnels Using Passive Thermography and Tapping

*Jungwon Huh*<sup>1)</sup>, *Van Ha Mac*<sup>2)</sup> and *Quang Huy Tran*<sup>3)\*</sup>

<sup>1)</sup> Department of Architecture and Civil Engineering, Chonnam National University, Gwangju 61186, Korea.

<sup>2)</sup> Division of Urban Transport and Coastal Engineering, Faculty of Civil Engineering, University of Transport and Communications, 3 Cau Giay, Hanoi, Vietnam.

<sup>3)</sup> Department of Civil Engineering, Nha Trang University, Khanh Hoa 57000, Vietnam.

\* Corresponding Author. E-Mail: [huytq@ntu.edu.vn](mailto:huytq@ntu.edu.vn)

### ABSTRACT

An unlined rock-blast tunnel constructed by the drill and blast method is susceptible to frequent deterioration, including sagging beds, water ingress and loose rock masses. Thus, assessing potential damages above the roadway that may impact the safety of tunnel users is of utmost importance. While tapping, a conventional non-destructive method, is typically used to predict sub-surface delamination, water ingress can be identified with the naked eye. In this research, we utilized a modern-technology approach called passive thermography, together with a high-resolution digital camera and tapping. The study encountered two primary challenges; namely, the absence of direct solar radiation during the inspection and the groove-exposed surface of the unlined tunnel. The results demonstrated that passive thermography was able to detect delaminated areas and water infiltration on the tunnel's walls and ceiling, even without direct sunlight. Large delaminated areas can be detected with just a 2°C change in atmospheric temperature twelve hours before testing. Additionally, the results of image post-processing significantly contributed to enhancing the results of passive thermography. The thermal image was processed into a grayscale image prior to HE processing, which enhances contrast by over 50%. The combination of tapping, digital camera and passive thermography was proven to be effective in periodically inspecting unlined rock tunnels, while significantly reducing time and cost.

**KEYWORDS:** Tunnel safety, Passive thermography, Old rock-cut tunnel, Hammer sounding, Non-destructive evaluation, Image post-processing.

### INTRODUCTION

Unlined rock tunnels are constructed underground using conventional mining techniques, where compressed air hammers are used for excavation, followed by drill and blast methods to break the rock (Japan Tunnelling Association, 2016; Centre d'Études des Tunnels, 2015). By this method, the medium to hard rock surface does not require permanent concrete or other supporting materials and is fractured and disturbed, as illustrated in Fig. 1. The disturbance typically extends one to two meters into the rock (Hung et al., 2009); Thus, the major drawback of unlined

tunnels is the potential for rock fragments to fall onto the roadway, as they become loose over time. To prevent this, loose rocks can be periodically removed from the tunnel roof using a backhoe, a steel liner roof can be installed or shotcrete can be applied to the tunnel walls and ceiling (Hung et al., 2009; Höfler and Schlumpf, 2004). However, to optimize capital allocation, regular maintenance to address minor damage is more cost-effective than investing in the complete renovation of the tunnel. Inspection of tunnels requires the evaluation of various functional aspects, including structural, mechanical, electrical, drainage, ventilation and operational considerations. The focus of this study is on the civil/structural aspect of a tunnel's capacity. Inspection parameters for the structural features of a tunnel include spalls, delaminated areas, cracks, joints

---

Received on 14/4/2023.

Accepted for Publication on 17/8/2023.

and moisture penetration, which are presented at an "element level" corresponding to defect condition states ranging from good to severe (Hung et al., 2009; Abdel-Halim and Al-Saad, 2018; Arizona Department of Transportation-Bridge Group, 2021).

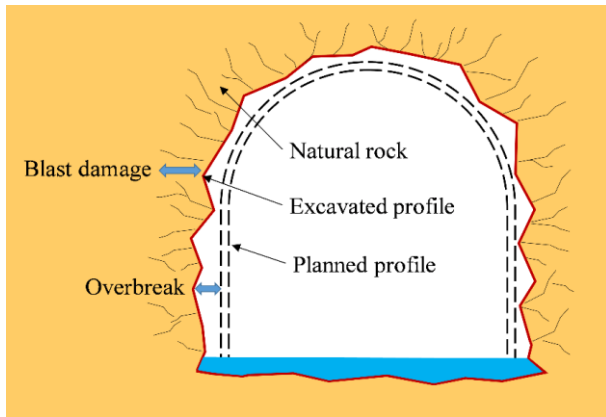


**Figure (1): Unlined rock-blast tunnel**

Assessment of the condition of tunnels presents a complex problem, which requires a combination of traditional - and advanced-technology methods. Modern non-destructive and non-contact evaluation methods, such as Light detection and ranging (LiDAR) sensors, Distance Measuring Instrument (DMI), High-resolution Video Imaging (HRVI), Ground Penetrating Radar (GPR) and Passive Infrared Thermography (PIRT), have been used for this purpose (IAEA, 2002; Gucunski et al., 2013; Huh et al., 2016; FHWA, 2016; Mac et al., 2019; Sjölander et al., 2023). LiDAR and HRVI data was

utilized to visually inspect a shotcrete tunnel in hard rock and reconstruct a 3D digital model (Sjölander et al., 2023; Sjölander, 2020). However, hidden damage and structural-condition detection cannot be achieved using these methods. GPR detection of grouting defects behind shield tunnel segments was studied for tunnels constructed in soft soil, such as saturated soft clay, silty soft soil, saturated sandy silt and silty sand (Peng et al., 2021). GPR was also employed to identify areas of delaminated and deteriorated concrete, voids behind the liner and areas of high moisture concentration within and behind the liner (Nako, 2018). PIRT was utilized for locating potential water-flow areas, detecting wet liner surfaces and identifying delaminated zones (Afshani et al., 2019). Mobile LiDAR and PIRT were also combined to map voids, debonding, delaminations, moisture and other defects behind or within tunnel linings (Treon, 2018). The study provided a proof of concept and implementation of surveying principles and thermal imaging in various Colorado tunnels. In 2018, a combination of HRVI, GPR and PIRT was studied and the survey results were typically presented in plan-view maps with colorized topography for each method (Nako, 2018). Box-type concrete and shield tunnels were investigated using PIRT to locate potential voids (Konishi et al., 2016). The main finding of this study is the ability to use PIRT with high accuracy when the temperature of the concrete surface exceeds that of the tunnel's interior atmosphere by 0.35°C. A brief summary of the aforementioned previous literature studies is presented in Table 1.

**Table 1. A summary of literature studies**

Non-destructive methods	Types of tunnels	Types of potential defects	Main findings	Authors
LiDAR and HRVI	- Shotcrete in hard rock - Concrete liner	Surface cracks, infiltrating water, leaching of concrete,...	Generate accurate dense point clouds, 3D models and surface defects	Sjölander, 2020; Sjölander et al., 2023
GPR	- Shield tunnel in soft soil	Grouting defects behind shield tunnel segments	A practical method for detecting grouting defects, but detection performance of GPR is affected by factors, such as antenna frequency, distance between transmission and reception, contact-coupling conditions and curing of the grouting layer	Peng et al., 2021

Non-destructive methods	Types of tunnels	Types of potential defects	Main findings	Authors
PIRT	Box-type and shield tunnels with concrete lining	Potential water flow areas, wet liner surfaces and delaminated zones	The temperature difference between the concrete surface and the tunnel air is more than 0.35°C, which is an ideal condition for detecting the voids with an approximate depth of 30 mm or less	Afshani et al., 2019
Mobile LiDAR and PIRT	- Rock-cut tunnel - Shotcrete tunnel - Concrete liner	Mapping voids, debonding, delaminations, moisture and other defects behind or within tunnel linings	The study provided a proof of concept and implementation of surveying principles and thermal imaging in various Colorado tunnels	Treon, 2018
A combination of HRVI, GPR and PIRT	- Concrete liner	Moisture detection, surface cracks and small spall, infiltrating water, debonded tile	Provide in –plan view maps with colorized topography for each method	Nako, 2018
PIRT	Box-type concrete and shield tunnels	Potential voids	- When the temperature of concrete surface exceeds that of tunnel inside atmosphere by 0.35°C or more, the detection rate of void in cut & cover tunnel became 76%. And when the size of void was larger than 10cm×10cm, the detection rate became 86% - When the inspections were performed under conditions with sufficient temperature difference by infrared thermometry in shield tunnels, the detection rate became over 95%	Konishi et al., 2016

According to Table 1, most of the studies focus on solving concrete lining tunnels, while there are not many studies on unlined rock tunnels. In addition, experiments in low light conditions old tunnels also face many difficulties when evaluating tunnel surfaces, such as distinguishing wet areas and black staining caused by carbon and pollution, evaluating uneven natural-rock surface conditions and the low temperature difference between tunnel walls and the atmosphere temperature inside the tunnel.

This paper aims to provide a comprehensive case study for an unlined rock-cut tunnel by combining the PIRT, high-resolution digital camera (HRDC), tapping and image post-processing methods. The study was first tested on specimens in the laboratory for theory verification. Then, the investigation was applied in the field for an old rock tunnel. HRDC was used to observe the rock surface, while HRDC, PIRT and tapping were combined to locate potential delaminated areas and water standing. Image post-processing was applied to

both digital and thermal images to effectively identify defects. Additionally, the white-balance method was applied to images captured in low light. These challenges are addressed and discussed in this study. The article is structured as follows: First, an introduction is presented. Then, the PIRT principle for the NDE aspect is explored. Thereafter, the experimental setup in the laboratory and the case study for detecting delamination and water ingress in an old rock-cut tunnel are described. The results are then presented and discussed. Finally, the conclusions are presented.

**Principles of Passive Infrared Thermography**

The passive infrared heat approach is simply described that after the structure is "sun-heated" for some time, if it has defects inside the structure, the temperature distribution on the surface of the structure will be different; when an infrared thermometer scans, it will discover the difference between the normal area and the "suspected" area of damage thanks to the uneven heat distribution on the surface. Undoubtedly, the defect for the infrared thermometer to find must be located near the surface, e.g. often no more than 10 cm for concrete unless the defect is substantial (Mac et al., 2019; Tran, 2021; Hiasa, 2016). Therefore, the infrared thermal method is available to measure the types of defects occurring in shallow areas near the outer surface, such as the cover layer of rebars for reinforced-concrete structures or the delamination zone for multi-layer material where the adhesive layer is peeling off

(Maldague, 2001; Usamentiaga et al., 2014).

The principle of this method is shown in Fig. 2. During the daytime, when solar radiation from the sun generates heat energy into the measuring object (e.g. concrete structure), the outside temperature will be greater than that of the structure's core. Thus, the heat flux flows through the object. When the heat flux encounters an obstacle boundary, such as cracks or delamination, it returns the heat to the surface, making the defective areas hotter than the surrounding regular locations, see Fig 2(a). Conversely, at night-time, when the outdoor temperature drops, it is most evident in cold regions; the heat in the structure which accumulated during the daytime will escape according to the principle of thermal balance. The defects will then impede the heat flow, causing the surface of the structure above the defective area to tend to be cooler than the surface of the surrounding undamaged areas, see Fig. 2(b) (Mac et al., 2019; Watase, 2013). Thus, the passive infrared heat experiment can be conducted both at daytime and night-time. The actual implementation may depend on the construction site conditions for deployment. The advantages of daytime measurement are low-cost labor and easiness to combine visual observations, but a disadvantage is crowded traffic. On the contrary, at night-time, an advantage is that the traffic density is low. However, comparing the thermal-image results with observing the exposure by the naked eye or digital images will not be easy. In addition, night-work costs will be higher.

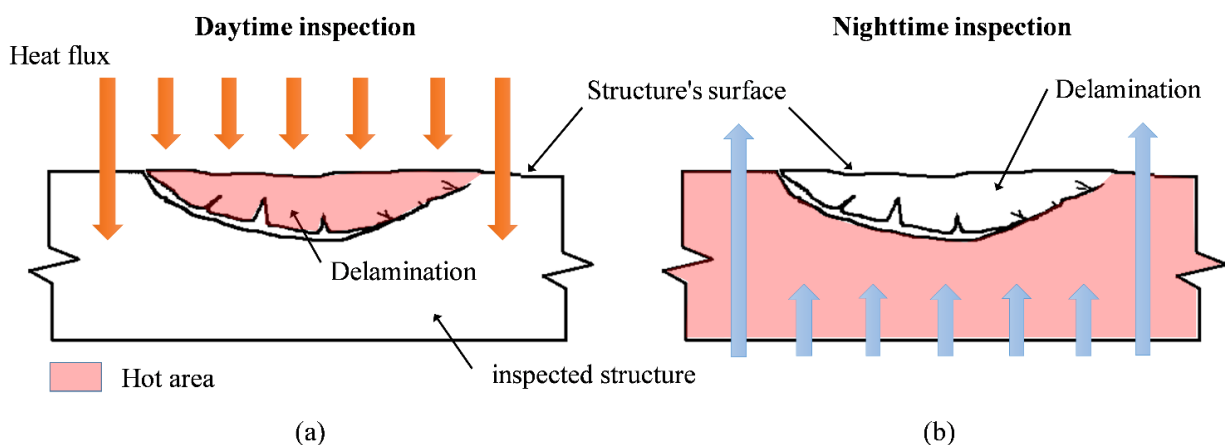


**Figure (2): Principle of detecting delaminated areas by PIRT, (a) Heat flux movement from outside into the structure, (b) Heat flux movement from the inner structure's core to outside**

### Detecting Delamination in Rock-cut Tunnel Lining Verification of PIRT Experiment in the Laboratory for Concrete Specimens

The laboratory tests were conducted in an outdoor setting to validate the effectiveness of using the PIRT for detecting delaminated areas. The concrete specimens were relocated to a car park and testing was conducted over the course of one week, as shown in Fig. 3(a) and 3(b). The results obtained demonstrate similar surface-temperature behavior as the PIRT principle, even under various weather conditions, such as sunny days, partial clouds and slight rainfall, as presented in Fig. 3(c) and 3(d). Previous studies have also demonstrated the efficacy of these analyses for concrete decks of a bridge

(Mac et al., 2019; Tran, 2021; Tran et al., 2023; Tran et al., 2018a). However, the effectiveness of PIRT may differ for a tunnel that is not exposed to direct sunlight. Additionally, various factors such as low contrast on thermal images due to lack of solar radiation, wind effects and grooved surfaces of the unlined rock can challenge the investigation. Thus, the laboratory tests serve as an excellent demonstration of site inspection for actual structures. Furthermore, the testing results indicate that temperature change is the key factor that enables infrared detection to be valuable. The infrared thermal device is ineffective if the outside atmosphere temperature and the temperature within the structure's core are balanced.

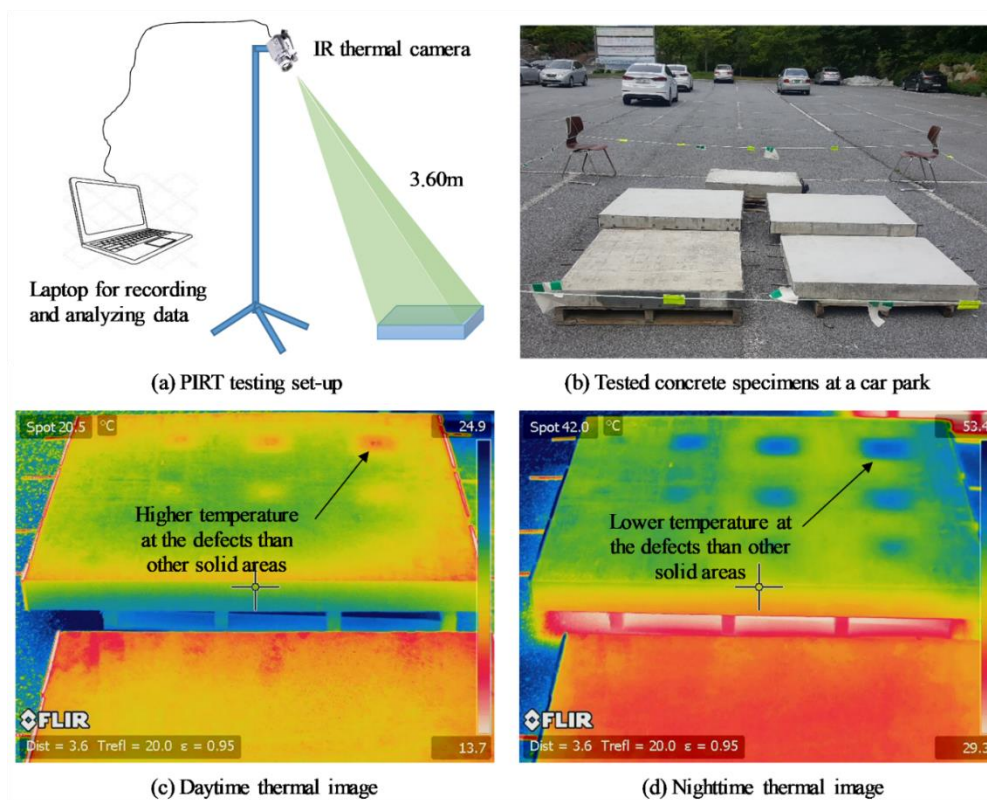
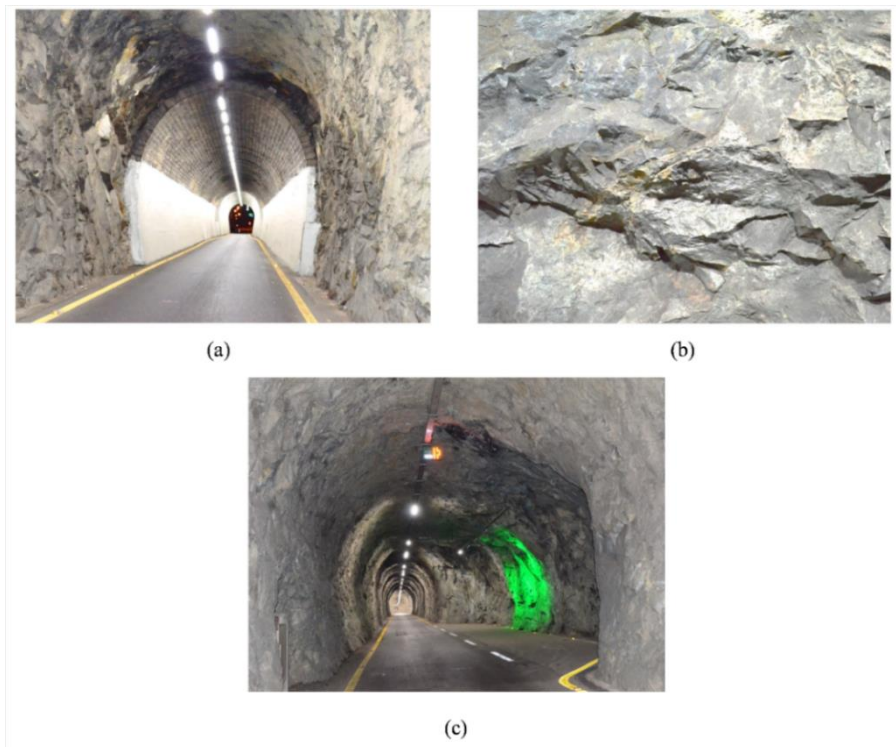


Figure (3): PIRT test for concrete specimens

### Case Study on an Old Rock-cut Tunnel

A case study was conducted on an old unlined rock-blast tunnel located in Yeosu, South Korea. Originally designed by Japanese engineers in 1926, the tunnel is a single-lane structure equipped with traffic lights at both ends for traffic control. Its dimensions are a length of 640m, a width of 4.5m and a height of 4.5m. The tunnel

was constructed without supporting the tunnel liner, with only the ends being consolidated using cement shotcrete and welded-wire fabric reinforcement. A widened section for car parking is also present, as illustrated in Fig. 4. Despite its age, the tunnel remains in a good condition, but a regular investigation is necessary to ensure the safety of its users.



**Figure (4): Inspected old rock-cut tunnel in South Korea; (a) Tunnel portal, (b) Unlined tunnel ceiling and (c) Widening road section for car parking at the middle of the tunnel**

**Testing Setup**

The testing was conducted during the spring season from 10:30 PM until early morning under night-time conditions. The ambient outdoor temperature and humidity during the testing period were approximately 16°C and 86%, respectively. To aid the technicians in visual observation and hammer sounding for the identification of delaminated areas, a lift truck was utilized, as depicted in Fig. 5(a). However, due to the limitations of the tapping method, only suspected locations were tested and random inspections were

carried out. In order to identify these "suspected" delaminated areas and water infiltration, a high-resolution, long-wavelength infrared thermal camera; namely, the FLIR SC660, was utilized. The IR camera, with a resolution of 640x480 pixels, 0.03°C sensitivity and ±1°C (1.8°F) accuracy, was found to be suitable for the inspection requirements. Further specifications of the IR camera are provided in Table 2 (FLIR SC660 Catalog, 2014), with environmental conditions during testing depicted in Table 3.

**Table 2. Technical data of high-resolution long-wavelength IR thermal camera (FLIR SC660 IR camera)**

Items	Parameters
IR resolution	640 x 480 pixels
Thermal sensitivity/NETD	<30 mK @ +30°C
Field of view (FOV)	24°×18°/0.3m
Spatial resolution (IFOV)	0.65 mrad
Focal plane array (FPA)	Uncooled micro-bolometer
Wavelength	7.5 ~ 13 μm
Temperature range	-40°C ~ +120°C
Accuracy	±1°C or ±1% of reading

**Table 3. Environmental conditions during the test**

Time	Day	Temperature (°C)	Weather	Wind speed (km/h)	Relative humidity (%)	Testing time
12:00	First day	18	Passing clouds	17	71	
15:00		18	Partly sunny	30	68	
18:00		17	Overcast	28	83	
21:00		16	Overcast	24	89	x
0:00	Second day	16	Passing clouds	22	85	x
3:00		16	Overcast	20	88	x
9:00		18	Passing clouds	13	71	

In this study, two processes were used to detect potential delaminated areas in the unlined rock-cut tunnel. The first process involved verifying the results of the tapping test with those of the PIRT technology, while the second process involved conducting PIRT in advance to locate suspected areas, followed by using the hammer-sounding test to confirm PIRT results. The second process was found to save time. The thermal images were processed using the ResearchIR software of the FLIR System Corporation (FLIR, 2012) and

Matlab as necessary. Both digital and thermal infrared cameras were positioned at a normal angle to the nominal surface of interest to achieve the most accurate results. Delamination depth cannot be detected, because the defect depth is just possible to Active Infrared Thermography (AIRT) in which the heat flux is controlled by external heat sources, such as halogen lamps or infrared heaters (Tran et al., 2018a; Tran et al., 2018b; Washer et al., 2009). Figure 5 illustrates photos of the tapping and PIRT methods during the inspection.

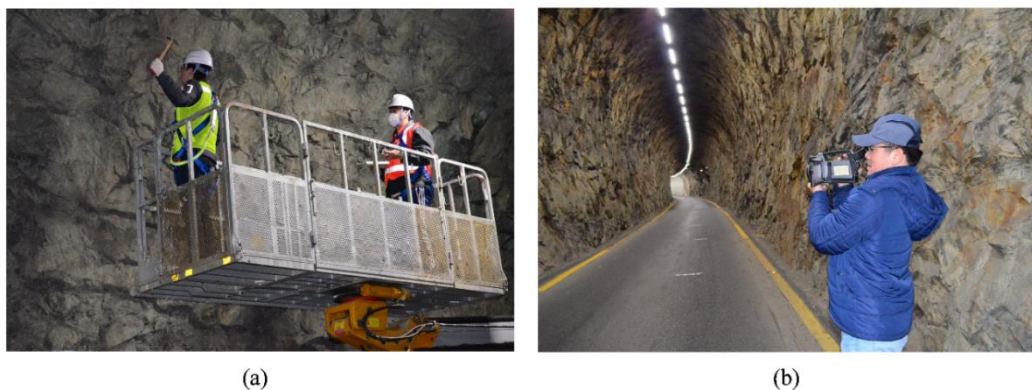


**Figure (5): Civil/structural inspection by (a) Tapping/hammer sounding test and (b) Passive infrared thermography**

The PIRT method faces challenges due to various parameters that affect the value of emissivity, such as materials (e.g. metal, concrete, rock), surface structure (rough or polished), geometry (grooves, cavities, ... etc.), observation direction, wavelength and temperature (Vollmer and Mollmann, 2010; Maldague, 2001; Bolleni, 2009). For natural-rock surfaces formed through the drill and blast method, the emissivity is generally high, making only the geometry of the surface, observation direction and atmospheric temperature

significant. When an object is observed from a direction normal to its surface ( $\delta=0$ ), it emits more radiation than when observed at oblique angles, as depicted in Fig. 6(a). To capture thermal images accurately, the FLIR System Corporation recommends using an angle not exceeding 60 degrees (FLIR, 2012). The surface geometry is linked to the surface structure and grooves can enhance emissivity in the direction perpendicular to the macroscopic surface, particularly for polished metal surfaces (Vollmer and Mollmann, 2010). This increase

occurs due to the contributions of direct and reflected emissions, as shown in Fig. 6(b). Moreover, the grooves, cavities and roughened surfaces of tunnels result in non-uniform emissivity distributions, making it difficult to differentiate between defective and non-defective areas. Finally, material properties change with temperature and emissivity can increase or decrease as temperature increases, depending on the material. For non-metal materials, heat exchange is slow and temperature can be assumed constant during inspections. A major challenge for technicians using the PIRT method is the need for direct solar radiation inside tunnels, resulting in low contrast in thermal images.

The present study suggests several potential solutions for mitigating the aforementioned factors. First, the infrared (IR) camera should be positioned perpendicularly to the tunnel walls to optimize the accuracy of the inspection. Second, it is recommended that highly experienced technicians are employed to conduct the inspections. Third, a combination of thermal imaging and high-resolution digital imaging should be utilized to account for surface grooves and to enhance the accuracy of the inspection. Finally, post-image processing may be utilized in cases where low thermal contrast is detected.

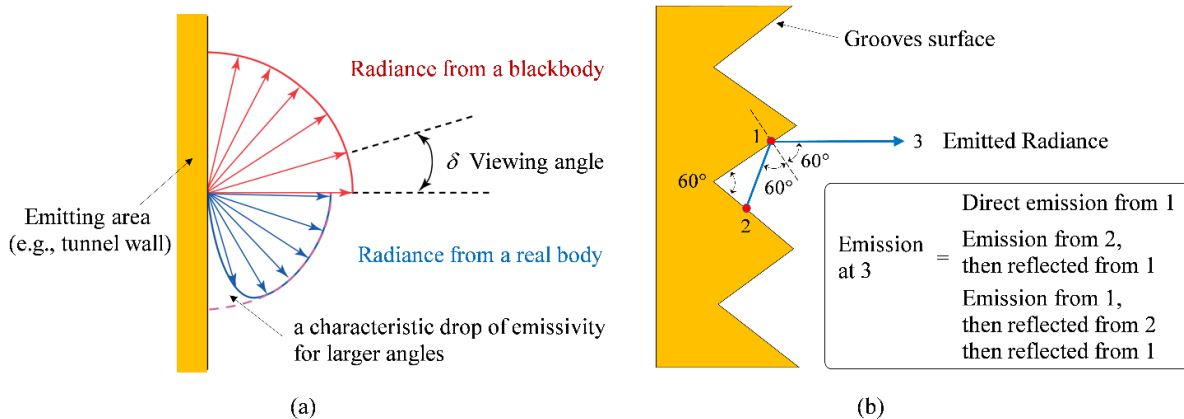


**Figure (6): Illustration of impact factors during PIRT testing;**  
**(a) Observation direction and (b) Geometry of the surface**

**RESULTS AND DISCUSSION**

Based on the aforementioned challenges, which include the surface structure and the geometry of the rock, observation direction and wavelength of the IR detector, temperature variations between the rock walls and the external environment and experimentation under low-light conditions, the results obtained from the combination of thermal imaging, high-resolution digital imaging, tapping and post-image processing were pronounced. This comprehensive approach facilitated the detection of sub-surface delamination and water penetration from groundwater in the rock. However, it should be noted that cracking could not be identified through these tests.

**Delamination Inspection**

The current experiment was designed to employ both thermal and high-resolution digital cameras to detect the

inside walls of the tunnel. The “questionable” areas have been warned to cross-check with the tapping method. The tunnel has two types of walls: shotcrete liner at the tunnel portals and natural groove surfaces, as previously described. In this project, shotcrete construction techniques were utilized to reinforce the tunnel portals, which are situated at both the entrance and the exit points. The shotcrete construction technique or sprayed concrete is taken through a hose and pneumatically projected at high velocity onto a surface, initially applied in 1907, invented by Carl Akeley (Höfler and Schlumpf, 2004). Conventional steel mesh, steel rods or fibers typically reinforce it. The cement in the sprayed-concrete mix acts as a "glue." Thus, the debonding between the concrete liner and steel mesh or between cement liner and natural rock might occur due to long-term operation and many factors, such as environment, groundwater, concrete-strength degradation and corrosion of reinforcement steel mesh. For the natural-

rock surface (in the middle of the tunnel), the delamination might be caused differently than for the shotcrete layer. Due to the failure pattern of rock, environmental conditions; e.g. temperature gradient, water penetration and external impact (e.g. traffic collision, reparation activities, ... etc.), minor cracks initially accelerate inside the rock, then develop into larger cracks or delamination. Inspection of elements above the roadway, such as potential spalls, falling objects and water standing, is crucial to ensure the safety of tunnel users.

The analysis of the data obtained from inspection of the shotcrete sections reveals that the PIRT technique is more effective in producing thermal contrast images

when compared to inspection performed at the midsection of the tunnel. This is attributed to the heat accumulation in the portal zone during the daytime, which is higher than that within the tunnel. Furthermore, there is a higher rate of heat exchange at the portal area compared to inside the tunnel. Examination of Fig. 7(a) and Fig. 7(c) indicates the presence of water stains at the location, but no significant issues were observed. However, the exposed steel mesh shown in Fig. 7(b) suggests the possibility of areas with debonding potential. Although thermal images were captured at this location as shown in Fig. 7(d), the results were not conclusive.

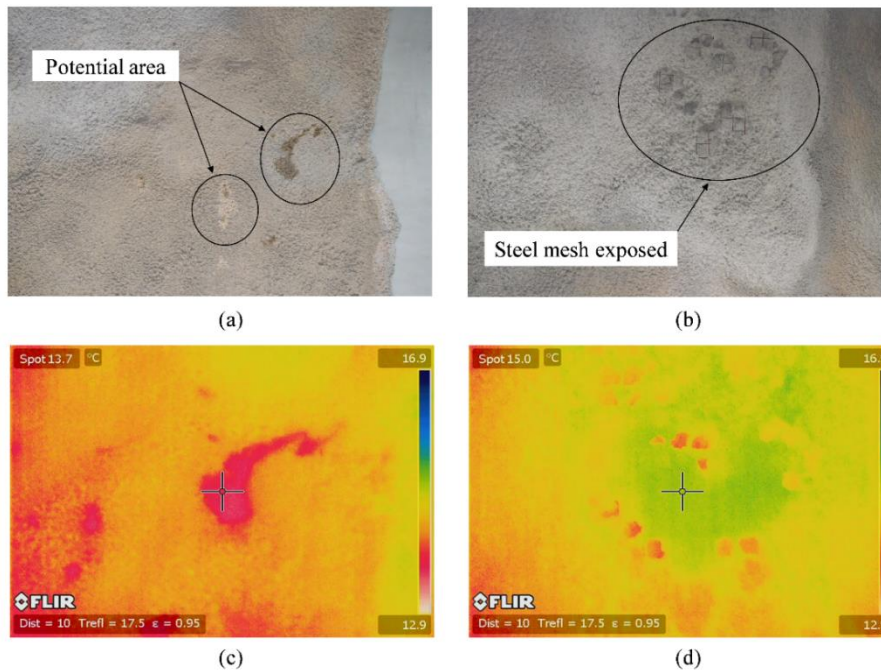


**Figure (7): Inspection results for the shotcrete sections at the tunnel portal, with potential areas of water accumulation and debonding presented in (a) and (b) for digital images and (c) and (d) for thermal images**

In Fig. 8, a post-processing analysis of the thermal image (Fig. 7d) was conducted using several common methods, including Histogram Equalization (HE), pseudo-color and white balance. Three different schemes were applied to detect potential hidden defects. The outcomes of the analysis demonstrate that the HE method was highly effective in identifying suspicious locations concealed beneath the steel layer. In particular, the difference between the potential area and the sound area is just around 6% in the original IR image, while

the difference increases to 14% after processing with HE, as shown in Fig. 9. The analysis also demonstrates that the difference reaches up to 50% when the analysis is applied to the grayscale image prior to HE processing. In other words, the sequential application of grayscale-image conversion and HE processing significantly enhances the probability of detecting delamination in the IR thermal image. HE is a technique that adjusts the image intensities to improve the overall contrast of an image. The underlying principle of this method relies on

the effective spread of the most frequently occurring intensity values.

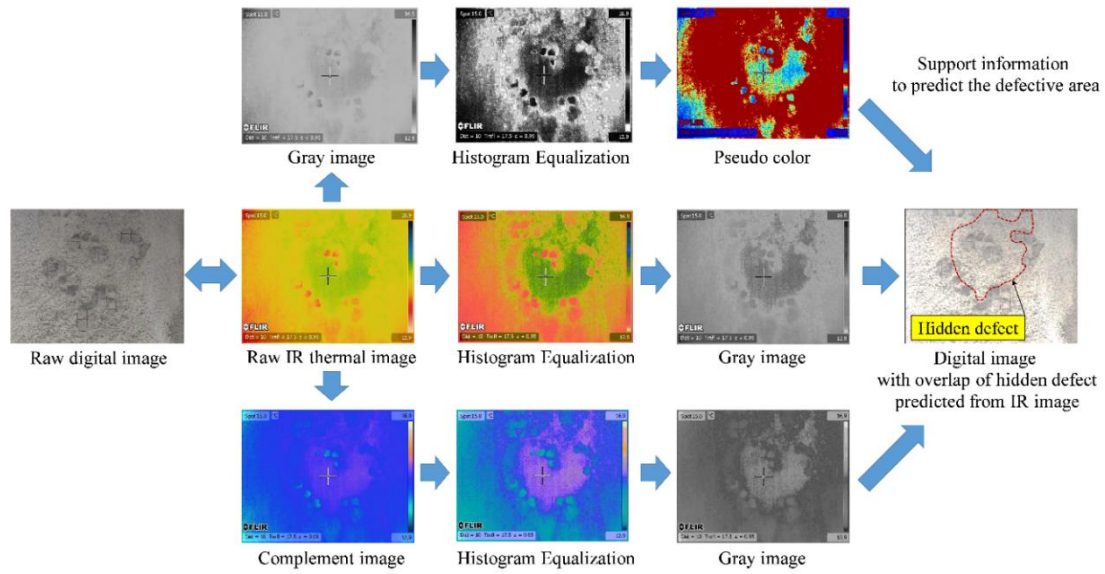


Figure (8): Post-processing of thermal images for the purpose of identifying potential hidden defects

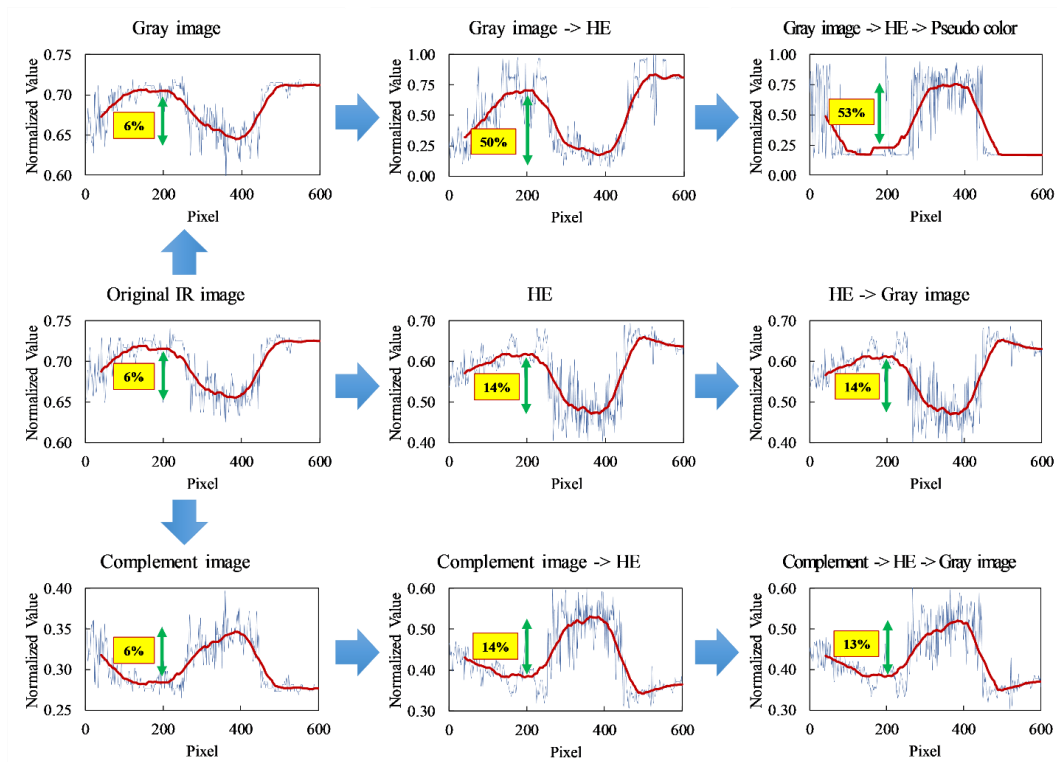


Figure (9): Analysis of the efficiency of image post-processing methods

Considering a discrete grayscale image  $\{x\}$ , the probability of an occurrence of a pixel of intensity level  $i$  (PDF) in the image is (Gonzalez and Woods, 2007):

$$p_x(i) = p(x = i) = \frac{n_i}{n}, \quad 0 \leq i < L \quad (1)$$

where  $p_x(i)$  is the image's histogram for pixel intensity value (or gray value)  $i$ ,  $L$  is the total number of gray levels in the image (e.g. for an 8-bit image,  $L = 256$  levels, which range from 0 to 255),  $n_i$  and  $n$  are the total number of pixels having the same gray level  $i$  and the

total number of pixels in the image, respectively. The cumulative distribution function (CDF) corresponding to  $p_x$  can be expressed as:

$$cdf_x(i) = \sum_{j=0}^i p_x(j) . \quad (2)$$

The general histogram equalization formula is:

$$h(i) = \text{round} \left( \frac{cdf_x(i) - cdf_{x_{\min}}}{(M \times N) - cdf_{x_{\min}}} \times (L - 1) \right) . \quad (3)$$

In this manner, the minimum and maximum values of the original image  $\{x\}$  have been transformed to 0 and 255, respectively. It should be noted that due to the application of the HE method, the new pixel values in the thermal image will represent different temperatures than those in the original image. Hence, it is cautioned against using the processed image for the purpose of temperature measurement.

The investigation revealed surprising results regarding the natural-rock surface inside the tunnel, where limited sunlight was present. Large delamination's were detected on the tunnel walls through thermal imaging, which may not have been detected by digital imaging, as shown in Fig. 10.

$$\text{Area of delamination} = \frac{\text{Number of pixels of delaminated area}}{\text{Number of pixels of test area}} \times 100 (\%) \quad (4)$$

### Water-penetration Detection

Groundwater intrusion is a significant issue in tunnels, as it can cause the deterioration and corrosion of the tunnel liner. The common solution to this problem involves sealing the liner with chemical or cementation grout. Therefore, it is necessary to identify a reliable method to measure the flow of water from a leak. In some instances, the use of PIRT can identify locations where water flow is significantly higher than in other areas. The fundamental principle behind the measurement of PIRT is based on the temperature gradient, where low temperatures suggest the presence of potential water standing. To supplement this method, high-resolution digital images should be used to observe the outer surface at questionable locations. The selection

Particularly, the background temperature of the rock walls ranges from 13.6°C to 14°C, while the temperature at the defective area is approximately 14.2°C. Thus, it is possible to detect the defect with a temperature difference of just 0.2°C, as can be seen in Figure 10(c). The roughness of the tunnel ceiling requires PIRT measurement results to be interpreted by a trained technician to ensure accuracy. Moreover, the change in temperature throughout the course of a day is also crucial, with larger changes being more favorable. In this study, the atmospheric temperature varied from 18°C to 16°C between noon and midnight (the time of testing). Therefore, we can conclude that it is possible to detect large delaminated areas with an approximate 2°C change in atmospheric temperature twelve hours before testing. Equation (4) is used to calculate the delamination percentage based on the results of the three methods: thermal imaging, high-resolution digital imaging and hammer sounding. The percentage of the delaminated area provides an indication of the lack of bond between the overlay and the underlying rock. This reference is based on the Standard Test Method for detecting delaminations in bridge decks using infrared thermography (ASTM D4788 2022) and hammer sounding (ASTM D4580 2007).

of grout depends on various factors, such as width, moisture content and potential for movement within the crack or joint. Therefore, inspection using PIRT is significant. Both thermal- and digital-imaging techniques are useful in detecting water infiltration in the rock section. Figure 11 illustrates digital and thermal images that show large areas of water standing at multiple tunnel locations. Notably, the temperature in the "dark" areas (where water is standing) in Fig. 11(b) is around 14°C, whereas the surrounding areas display a temperature of approximately 15°C, as shown in the thermal profile in Fig. 11(c), indicating the presence of water. Similar to delamination, the percentage of water standing area can be estimated from thermal images using Equation (5).

$$\text{Area of water infiltration} = \frac{\text{Number of pixels of water infiltration area}}{\text{Number of pixels of test area}} \times 100 (\%) . \quad (5)$$

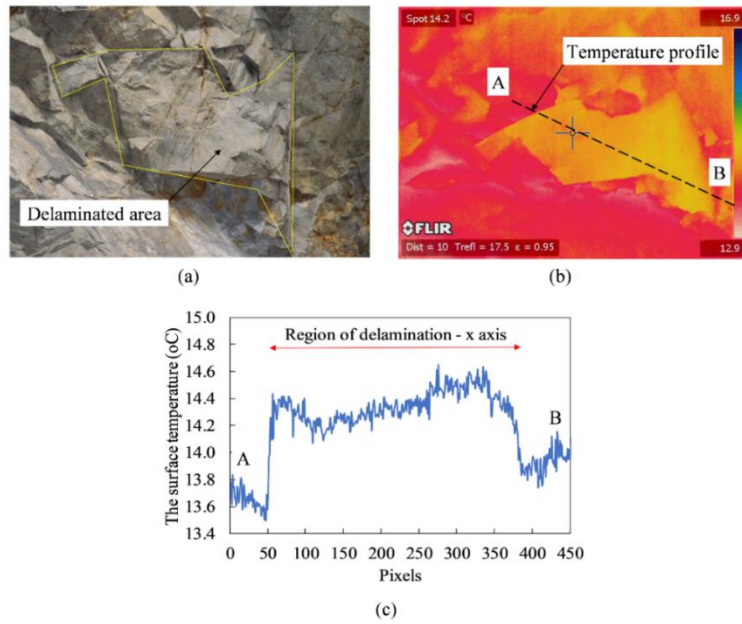


**Figure (10):** Detection of delamination in exposed rock-surface areas through (a) High-resolution digital imaging, (b) Thermal imaging and (c) The surface temperature profile crossing the delaminated area

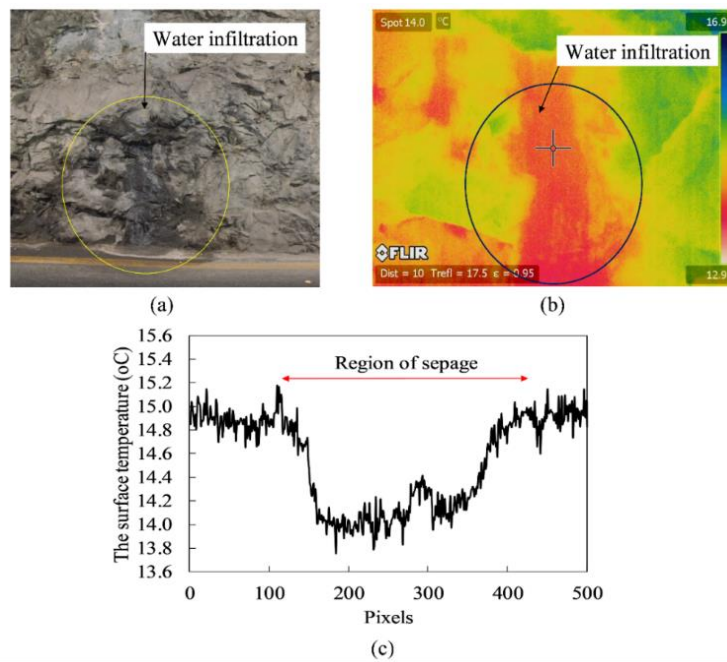


**Figure (11):** Water infiltration detection, (a) Digital image, (b) Thermal image and (c) The surface temperature profile crossing the area of water standing

In low-light conditions, it is challenging to detect water standing in a dark space, particularly with the reflection of neon lights, as shown in Fig. 12(a). To solve this issue, the digital image obtained by HRDC (Fig. 12a) was subjected to a white-balance process,

resulting in Fig. 12(b), which allows the recognition of two dark areas. The thermal image (Fig. 12c) obtained by PIRT was processed into a grayscale image prior to HE processing, producing Fig. 12(d), which enhances the contrast by over 50%. The processing of both the

digital and thermal images helps distinguish the wet areas and black stains. As a result, the area of water

infiltration can be accurately located.

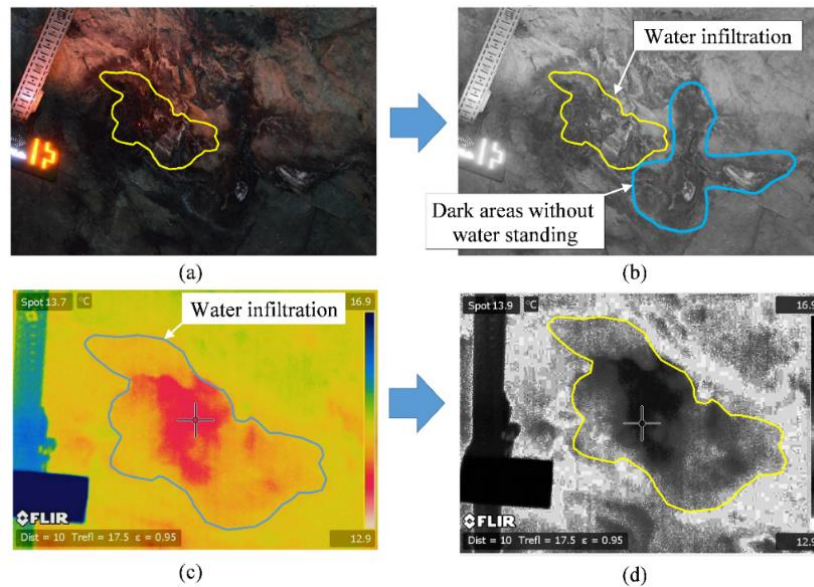


**Figure (12): Image-processing techniques employed to detect water infiltration, where (a) depicts the raw digital image, (b) displays the white-balance analysis for photo (a), (c) shows the raw thermal image and (d) presents the histogram-equalization (HE) analysis for the gray image of photo (c)**

## CONCLUSIONS

In this study, an investigation was conducted on an old rock-blast tunnel to locate sub-surface delamination and water infiltration. To achieve this, a comprehensive process was applied, including PIRT, a high-resolution digital camera, tapping and image post-processing methods, with laboratory verification and field application. The combination of tapping, a digital camera, PIRT and image post-processing methods has been demonstrated to be effective, time-efficient and cost-efficient in the periodic inspection of unlined rock tunnels.

The main conclusions of this study are as follows:

1. Temperature change is crucial for the effectiveness of infrared detection. This study concludes that large delaminated areas can be detected with just a 2°C change in atmospheric temperature twelve hours before testing. If the outside atmospheric temperature is similar to the temperature inside the rock's core, the infrared thermal device becomes ineffective.
2. Image post-processing techniques can be effectively employed for tunnel inspection, such as Histogram

Equalization, pseudo-color and white balance. Histogram Equalization analysis can effectively process the thermal images to detect hidden sub-surface defects. The thermal image was processed into a grayscale image prior to HE processing, which enhances the contrast by over 50%. White-balance analysis can lighten dark digital images captured in low-light conditions, while pseudo-color can colorize the images to aid technicians and engineers in easily interpreting the deteriorations.

3. The processing of both the digital and thermal images using gray image and HE helps distinguish wet areas and black stains, accurately locating the areas of water infiltration in low-light condition.

## Recommendations

Based on the efficiency of this study, further research should be conducted in the following directions:

- Studying the effect of environmental changes, including atmospheric temperature and relative humidity, on the ability to detect sub-surface defects when using PIRT.
- Conducting research on measuring the depth of

defects using the Active Infrared Thermography method with an external heat source and a windbreak system.

### Conflict of Interests

The authors confirm that there is no conflict of interests relevant to the content of this article.

## REFERENCES

- Abdel-Halim, M.A.H., and Al-Saad, Z. (2018). "Deterioration and damage evaluation of the monument of Qasr al-Bint, Petra-Jordan and a suggested conservation program". *Jordan Journal of Civil Engineering*, 12 (3), 424-434.
- Afshani, A., Kawakami, K., Konishi, S., and Akagi, H. (2019). "Study of infrared thermal application for detecting defects within tunnel lining". *Tunnelling and Underground Space Technology*, 86, 186-197.
- Arizona Department of Transportation-Bridge Group. (2021). "Tunnel inspection guidelines". Arizona Department of Transportation.
- ASTM D4580. (2007). "Standard practice for measuring delaminations in concrete bridge decks by sounding". ASTM International.
- ASTM D4788. (2022). "Standard test method for detecting delaminations in bridge decks using infrared thermography". ASTM International.
- Bolleni, K.N. (2009). "Environmental effects on sub-surface-defect detection in concrete structures using infrared thermography". University of Missouri, Columbia.
- Centre d'Études des Tunnels. (2015). "Book 1: From disorder to analysis, from analysis to rating in road-tunnel civil-engineering inspection guide". Centre d'Études des Tunnels, Bron, France.
- FHWA. (2016). "Federal highway administration research and technology: Non-destructive evaluation (NDE) web manual". <https://fhwaapps.fhwa.dot.gov> (Dec. 9, 2016).
- FLIR. (2012). "The ultimate infrared handbook for R&D professionals". FLIR Systems, Inc.
- FLIR SC660 Catalog. (2014). "Technical data of FLIR SC660 infrared camera". FLIR System, Inc.
- Gonzalez, R., and Woods, R. (2018). "Digital image processing". 4<sup>th</sup> Edn., Pearson, New York.
- Gucunski, N., Imani, A., Romero, F., Nazarian, S., Yuan, D., Wiggenhauser, H., Shokouhi, P., Taffe, A., and Kutrubes, D. (2013). "Non-destructive testing to identify concrete bridge deck deterioration". Report S2-R06A-RR-1, Transportation Research Board, Washington, D.C.
- Hiasa, S. (2016). "Investigation of infrared thermography for sub-surface-damage detection of concrete structures". University of Central Florida, Orlando, Florida.
- Höfler, J., and Schlumpf, J. (2004). "Shotcrete in tunnel construction". Sika, Inc.
- Huh, J., Tran, Q. H., Lee, J., Han, D., and Yim, S. (2016). "Experimental study on detection of deterioration in concrete using infrared-thermography technique". *Advances in Materials Science and Engineering*, Article ID 1053856, 12.
- Hung, C., Monsees, J., Munfa, N., and Wisniewski, J. (2009). "Technical manual for design and construction of road tunnels: Civil elements (FHWA-NHI-10-034)". FHWA, Washington, D.C., 20590.
- IAEA. (2002). "Guidebook on non-destructive testing of concrete structures". IAEA, Austria.
- Japan Tunnelling Association. (2016). "Tunnelling activities in Japan 2016". Japan Tunnelling Association, Tokyo, 104-0045.
- Konishi, S., Kawakami, K., and Taguchi, M. (2016). "Inspection method with infrared thermometry for detecting void in sub-way tunnel lining". *Procedia-Engineering*, 165, 474-483.
- Mac, V.H., Tran, Q.H., Huh, J., Doan, N.S., Kang, C., and Han, D. (2019). "Detection of delamination with various width-to-depth ratios in concrete bridge deck using passive IRT: Limits and applicability". *Materials*, 12, 3996.
- Maldague, X.P. (2001). "Theory and practice of infrared technology for non-destructive testing". John Wiley & Sons, New York.

### Acknowledgments

This work was supported by a grant from the National Research Foundation of Korea (NRF) funded by the Korean government (MSIT) (No. 2021R1A2C1005587). The authors acknowledge the contributions of the research-team members in the SA-NDE-T Lab at the Civil Engineering Department of Nha Trang University.

- Nako, A. (2018). "Final report on the non-destructive inspection of the tooth rock and vista ridge tunnels". Penetradar Corporation, NY 14304.
- Peng, M., Wang, D., Liu, L., Shi, Z., Shen, J., and Ma, F. (2021). "Recent advances in the GPR detection of grouting defects behind shield tunnel segments". *Remote Sensing*, 13, 4596. doi.org/10.3390/rs13224596
- Sjölander, A., Belloni, V., Ansel, A., and Nordström, E. (2023). "Towards automated inspections of tunnels: A review of optical inspections and autonomous assessment of concrete-tunnel linings". *Sensors*, 23, 3189. doi.org/10.3390/s23063189
- Sjölander, A. (2020). "Structural behaviour of shotcrete in hard-rock tunnels". PhD Thesis, KTH Royal Institute of Technology, Stockholm, Sweden.
- Tran, Q. (2021). "Passive and active infrared-thermography techniques in non-destructive evaluation for concrete bridge". AIP Conference Proceedings, 2420, 050008.
- Tran, Q., Dang, Q., Pham, X., Truong, T., and Nguyen, T. (2023). "Passive infrared-thermography technique for concrete structures health investigation: Case studies". *Asian Journal of Civil Engineering*, 24, 1323-1331.
- Tran, Q., Huh, J., Kang, C., Lee, B., Kim, I.-T., and Ahn, J.-H. (2018a). "Detectability of sub-surface defects with different width-to-depth ratios in concrete structures using pulsed thermography". *Journal of Non-destructive Evaluation*, 37 (32), 1-10.
- Tran, Q., Huh, J., Mac, V., Kang, C., and Han, D. (2018b). "Effects of rebars on the detectability of subsurface defects in concrete bridges using square-pulse thermography". *NDT and E International*, 100, 92-100.
- Treon, M. (2018). "Non-destructive testing and monitoring of tunnels with mobile LiDAR and thermography (SHRP2-Project R06G)". Colorado Department of Transportation, Report No. CDOT-2018-18, Denver, CO 80204.
- Usamentiaga, R., Venegas, P., Guerediaga, J., Vega, L., Molleda, J., and Bulnes, F.G. (2014). "Infrared thermography for temperature measurement and non-destructive testing". *Sensors*, 14, 12305-12348.
- Vollmer, M., and Mollmann, K.P. (2010). "Infrared thermal imaging: Fundamentals, research and applications". Viley-VCH, Weinheim, Germany.
- Washer, G.A., Fenwick, R.G., and Bolleni, N.K. (2009). "Development of hand-held thermographic inspection technologies". MoDOT, Missouri.
- Watase, A. (2013). "Non-destructive evaluation of concrete structures using high-resolution digital-image and infrared-thermography technology". University of Central Florida, Orlando, Florida.